

14-93
E7452

77

NASA Technical Memorandum 105936
AIAA-93-0599

Acoustic Mode Measurements in the Inlet of a Model Turbofan Using a Continuously Rotating Rake: Data Collection/ Analysis Techniques

David G. Hall
Sverdrup Technology, Inc.
Brook Park, Ohio

and

Laurence Heidelberg and Kevin Konno
Lewis Research Center
Cleveland, Ohio

Prepared for the
31st Aerospace Sciences Meeting
sponsored by the American Institute of Aeronautics and Astronautics
Reno, Nevada, January 11-14, 1993



ACOUSTIC MODE MEASUREMENTS IN THE INLET OF A MODEL TURBOFAN USING A CONTINUOUSLY ROTATING RAKE: DATA COLLECTION/ANALYSIS TECHNIQUES

David G. Hall
Sverdrup Technology, Inc.
Lewis Research Center Group
Brook Park, Ohio 44142

Laurence Heidelberg and Kevin Konno
National Aeronautics and Space Administration
Lewis Research Center
Cleveland, Ohio 44135

Abstract

This paper documents the rotating microphone measurement technique and data analysis procedures used to determine circumferential and radial acoustic mode content in the inlet of the Advanced Ducted Propeller (ADP) model. Circumferential acoustic mode levels were measured at a series of radial locations using the Doppler frequency shift produced by a rotating inlet microphone probe. Radial mode content was then computed using a least-squares curve fit with the measured radial distribution for each circumferential mode. The rotating microphone technique is superior to fixed-probe techniques because it results in minimal interference with the acoustic modes generated by rotor-stator interaction. This effort represents the first experimental implementation of a measuring technique developed by T.G. Sofrin. Testing was performed in the NASA Lewis Low Speed Anechoic Wind Tunnel at a simulated take-off condition of Mach 0.2. This paper includes the design of the data analysis software and the performance of the rotating rake apparatus. The effect of experimental errors is also discussed. The ADP model was designed and built by the Pratt & Whitney Division of United Technologies.

Introduction

Acoustic testing of the ADP model was conducted between October 1990 and April 1991 in the NASA Lewis Low Speed Anechoic Wind Tunnel. Woodward, et al.¹ documented this testing, concentrating on far-field noise measurements with some results from the rotating rake. The present report will provide more detail on the rotating rake measurement technique. A related publication² provides a detailed description of the rotating rake test results.

The ducted propeller represents a hybrid technology, providing the structural and acoustic benefits of the high bypass ratio turbofan while retaining much of the

efficiency and aero-acoustic performance of the unducted propeller. In particular, the ADP engine is designed to allow in-flight adjustment of rotor blade pitch angles to provide reverse thrust. This eliminates the weight and drag penalties inherent in conventional thrust reverser hardware. Engine fan tones are an important component in overall aircraft noise. These tones are a result of the interaction between rotor blade wakes and the fixed stator vanes. A typical analysis of the spinning pressure field in the duct proceeds by evaluating the periodic (modal) variations in the circumferential and radial directions.³

Attempts to measure the modal content of the discrete, coherent sound in a fan inlet duct have been made in the past with limited success. The rotating rake method employed in this test was developed by T.G. Sofrin and previously documented in Ref. 4.

This method is unique because accurate measurement of the modal content is possible despite the contaminating effect of the wake created by the presence of the pressure measurement rake directly upstream of the rotor. The acoustic signal resulting from rake-rotor interaction appears as a circumferential mode with order equal to the number of rotor blades (the rotor-locked mode). This mode becomes cut-on in a ducted fan only when the rotor blade tip speed becomes supersonic. The analysis for a fan with subsonic tip speed (such as the ADP model) proceeds by ignoring the rotor-locked mode. During the NASA Lewis ADP tests, rotating rake measurements were made with three different inlet geometries and two stator vane configurations. Some testing was also performed with fixed inlet rods to generate a known inlet distortion pattern (and therefore a predictable modal content).

Processing of the pressure data was performed in two steps. First, a high resolution spectral analysis was used with time domain averaging to obtain the circumferential modal content at a series of radial locations. Then, these circumferential results were used as the input to a

program which calculated radial modes from a least-squares curve fit having eigenfunctions composed from Y and J type Bessel functions. This program also had the capability to simulate the inlet pressure field with user-selected modal coefficients and add random noise to permit analysis of the effect of experimental errors on the rotating rake method.

The main body of this paper is divided up into six major sections following this introduction. The first section presents background information on the rotating rake technique. The second section describes the experimental apparatus and procedures. The third section provides a mathematical basis for radial and circumferential mode decomposition. The fourth section discusses experimental errors and their impact on the data analysis. The fifth section documents "lessons learned" and presents recommendations for future research. The sixth and final section contains concluding remarks.

Background

The material in the following section is intended to provide the reader with a detailed understanding of the pressure measured by a rotating microphone in the inlet of a ducted fan. In concept, the rotating pressure probe uses doppler shift physics to separate circumferential rotating mode orders. This analysis, which was originally published in Ref. 4, is presented below for the sake of completeness.

First, the mathematical expression for the acoustic pressure at a fixed point in the duct will be developed from a modal viewpoint. This description will then be extended to describe the pressure measured at a point which rotates, with speed proportional to the fan rotation. It will be shown that each active circumferential mode induces a signal at a unique frequency. The effect of the rake wake contamination will then be discussed. A mathematical analysis will be presented to show that the contamination produces a spurious circumferential mode with order equal to the number of fan blades. This rotor-locked mode can not exist for fans with subsonic tip speed (such as the ADP model). The spectral signal corresponding to this mode, which occurs at a distinct frequency, is simply ignored in the final modal analysis.

General Concept

The acoustic pressure, at a fixed radial location in a plane which is perpendicular to the duct axis, may be described as follows. θ is the angular location in the circumferential direction:

$$P(\theta, t) = \operatorname{Re} \left[\sum_{n=0}^{\infty} \sum_{m=-\infty}^{\infty} C_m^n \exp i * (m * \theta - n * \omega * t) \right] \quad (1)$$

where

- P pressure
- t time
- ω fan shaft speed
- m circumferential wave order
- n shaft speed harmonic number
- C mode coefficient

The complex circumferential mode coefficient (C) gives amplitude and phase at a frequency equal to a harmonic of the fan speed ω . For a fan with B evenly spaced, symmetric blades and subsonic tip speed, the significant values for n are B, 2B, 3B. . . . Positive values for m denote modes which are rotating in the same direction as the fan, while negative values indicate rotation in the opposite direction.

Now consider the pressure measured at a point which is rotating in the circumferential direction. The term θ in Eq. (1) is replaced by $\Omega * t$, where Ω is the angular speed of rotation:

$$p(\theta, t) = \operatorname{Re} \left\{ \sum_{n=0}^{\infty} \sum_{m=-\infty}^{\infty} C_m^n \exp -i * [(n * \omega - m * \Omega) * t] \right\} \quad (2)$$

The frequency of this signal for a given m-number (circumferential mode) at the blade passing frequency ($n = B$) is thus:

$$\text{freq} = B * \omega - m * \Omega \quad (3)$$

In the nonrotating case, the circumferential (m) modes produce signals only at the blade passing frequency (BPF) and its harmonics. In the rotating case, the frequency of the signal produced by a given m-mode is shifted away from the BPF. The degree of shift depends on the order of the m-mode and the angular velocity of the measuring device. For example, suppose we are completing one 360° survey of the duct during the time it takes for the fan to complete 100 revolutions. Thus, $\omega = 100 * \Omega$, and Eq. (3) may be rewritten as:

$$\text{freq} = \omega (B - m/100) \quad (4)$$

In this case, the probe is rotating at a speed which is directly proportional to the fan speed. This proportionality is critical. The frequency of the signal produced by the $m = 1$ circumferential mode will appear with a frequency shift of 0.01 shaft orders. The $m = 2$ mode will have a frequency shift of 0.02 and so forth. Furthermore, m -modes with negative numbers will have unique frequency shifts in the opposite sense. A typical spectrum (from a test with the ADP model) is shown in Fig. 1. This spectrum contains clusters of closely spaced tones, centered at frequencies of $B, 2B, 3B, \dots$, etc. The blade passing frequency for this case was 2880 Hz.

Contamination Due to the Wake of the Rotating Microphone

The above discussion ignores the effect of the wake generated by the presence of the microphone in the duct. This section will analyze the effect of that wake and show that it does not interfere with mode measurements in most cases.

The interaction noise field generated by the presence of a fixed inlet distortion may be expressed as a superposition of frequency harmonic terms as follows:

$$P_L^n(\theta, t) = \operatorname{Re} \left\{ C_L^n \exp -i * [(n \pm L) * \theta - n * \omega * t] \right\} \quad (5)$$

where

P pressure

θ angular location of the distortion in the circumferential direction

L circumferential spatial harmonic number for the wake

ω fan speed, rad/sec

n $B, 2B, 3B, \dots$

If the distortion rotates slowly, with speed Ω , the frequency at which the rotor cuts through the distortion-induced wake changes by an additive factor of $(L * \Omega)$ and the noise field may be written as follows:

$$P_L^n(\theta, t) = \operatorname{Re} \left\{ C_L^n \exp i * [(n \pm L) * \theta - (n * \omega \pm L * \Omega) * t] \right\} \quad (6)$$

To determine the time signal sensed by a microphone which rotates with the distortion, we make the substitution $\theta = \Omega * t$. After cancelling like terms, the result-

ing expression for the time signal generated by the rake wake distortion is:

$$P_L^n(t) = \operatorname{Re} \left[C_L^n \exp i - n(\omega - \Omega)t \right] \quad (7)$$

where

n $B, 2B, 3B, \dots$

This implies that the signal generated by the rotating microphone disturbance appears only at a single frequency, equal to the blade passing tone minus B times the microphone speed. It is also important to note that this frequency is not a function of L , the wake spatial harmonic number. This is a critical result. The interpretation given to a signal at this frequency in the "tonal cluster" of a rotating microphone measurement is a circumferential mode of order B (equal to the number of fan blades). This mode, corresponding to the direct rotor field, cannot propagate in a ducted fan with subsonic tip speed (such as the ADP model). During analysis of the rotating measurement data from such a fan, the signal component at the frequency corresponding to $m = B$ is simply ignored. In cases with supersonic fan tip speed, the analysis is contaminated by the spurious microphone wake only for the $m = B$ mode, which may propagate.

Apparatus

The rotating rake assembly provided a precise circumferential drive for the microphone rake. A photograph of the rotating pressure probe installed on the ADP model in the NASA Lewis 9- by 15-Foot Anechoic Wind Tunnel is shown in Fig. 2. As shown in the cross-sectional sketch of Fig. 3, this was accomplished by mounting the rake, facing inward, from a large ring gear. The ring gear was driven by a stepping type electric motor coupled through a pinion gear. The ring gear had a sufficient diameter to assure that only the transducer rake interacted with the fan inflow. The ring gear revolved on a precision ball bearing track which was, in turn, secured to the test model. The pinion/ring gear ratio was 16:110. The rake was equipped with five pressure transducers acting as microphones. These transducers, model 8507C-5, were supplied by the Endevco/Allied Signal Company with a nominal sensitivity of $8.7 \mu\text{V}/\text{Pa}$ ($0.060 \text{ V}/\text{psi}$), an operating range of 0 to 34 482 Pa (0 to 5 psi), and a nominal diameter of 2.34 mm (0.092 in.).

Telemetry and signal conditioning electronics were attached to the rotating rake/gear. The telemetry system used FM encoding to transmit the rake pressure signals to an adjacent antenna. The five rake transducer

signals were demodulated using standard telemetry receivers and recorded on FM analog tape using IRIG Wide Band Group I format at a speed of 30 in./sec. The fan and ring gear were each equipped with 1/rev tachometer pickups which were recorded on the analog tape along with an IRIG B time code signal. Information from these tachometer pickups was used to precisely control the rake rotational speed as a fraction of the fan rotor speed.

The ADP model was configured with three different inlets and two different stator vane numbers during rotating rake testing. The rake was operated at two different radial immersions for each model configuration, requiring a total of 10 test runs. Shim pieces of varying thickness were inserted between the rake arm and the ring gear to adjust the radial location of the rake. These shims were designed to insure that when the rake was changed from inner to outer immersion, transducer #1 occupied the location vacated by transducer #2. During the initial data analysis, the results from these two transducers were carefully examined to verify that model operating conditions were comparable. During final data analysis, the data from the inner and outer immersion runs were merged prior to circumferential (spectral) analysis, giving nine independent radial measurement locations. The data for the repeated radial location (#1 Inner/#2 Outer) were determined by taking a complex average of the two spectra.

A block diagram of the rake control system is shown in Fig. 4. Testing was conducted by first bringing the ADP model up to operating speed. The ring gear drive motor was then activated and manually brought up to a speed near the desired operating speed. The automatic speed control system was then engaged to establish a tight synchronization between fan and rake. The initial design of the rake control system included a fan/rake speed ratio of 200:1. This was modified to 250:1 during development because the stepper motor tended to stall at high fan speeds.

During development of the apparatus, the fan/rake synchronization requirement was stated as follows: With a fan/rake speed ratio of 250:1, the fan would (ideally) rotate through $90\,000^\circ$ while the rake rotated through 360° . The control system was designed to provide an actual fan revolution of $90\,000 \pm 15^\circ$ while the rake rotated once. This was accomplished by modulating the speed of the rake drive motor. The ADP model was powered by a NASA air turbine drive motor, operating from the NASA Lewis 450-psi air supply system. Air turbine speed was set using a system of pneumatic regulators and valves. The fan speed tended to vary randomly over a small range (approximately ± 0.2 percent) during testing. This variation had to be tracked precisely by the rotating rake control

system in order to implement corresponding changes in rake speed. Details may be found in Ref. 5.

Data Processing Algorithms

This following section describes the data processing function for this experiment in detail. First, the circumferential modal decomposition is discussed. A high resolution spectrum analysis was used to compute the magnitude and phase of each circumferential mode at a series of radial locations. The radial mode analysis was performed using the radial distribution data for each circumferential mode as the input to a least-squares curve fitting program. Bessel eigenfunctions were used in calculating the radial coefficients.

Circumferential Mode Analysis

The pressure measurement data was digitized using an angle clock to generate 128 samples for each fan revolution. Fan set speed varied from 6600 to 12 000 rpm, so the actual sample rate varied from 14 080 to 25 600 Hz. The requirement for this experiment was to attempt to analyze the tone clusters centered at the BPF frequency as well as those at $2 * \text{BPF}$ and $3 * \text{BPF}$. With 16 fan blades, $3 * \text{BPF}$ equates to a center frequency of 9600 Hz for the maximum speed case of 12 000 rpm. Analog low pass anti-aliasing filters were used with cutoffs set to 10 kHz during digitizing.

The length of each time averaged pressure ensemble was selected according to the required spectral resolution. The frequency spread between adjacent tones in the tone cluster centered at BPF was determined from the fan/rake speed ratio to be $(\text{fan speed})/250$. This corresponds to a frequency spread of 0.8 Hz at the highest fan speed and to a spread of 0.56 Hz at the lowest speed. It was decided that at least two to three frequency points were required between adjacent tones. A further requirement was to form the averaged pressure ensembles from an integral number of rake revolutions. An ensemble consisting of five rake revolutions was chosen. This provided a frequency resolution varying from 0.2 Hz (at 12 000 rpm) to 0.112 Hz (at 8400 rpm). The use of the angle clock, with a constant 128 samples per fan revolution, resulted in a constant spectral resolution of 0.0078 shaft orders. The number of samples in a single ensemble was calculated as follows:

$$\begin{aligned} \# \text{ samples} &= (\# \text{ samples/fan rev}) * (\# \text{ fan revs/rake} \\ &\quad \times \text{ rev}) * (\# \text{ rake revs/ensemble}) \\ &= 128 * 250 * 5 = 160\,000 \end{aligned} \quad (8)$$

Time domain data was collected in files corresponding to 20 consecutive rake revolutions, yielding 640K data points per channel. From this, 16 overlapping ensembles were extracted (each ensemble containing 5 rake revolutions) and averaged. The once-per-revolution tachometer pickups from the rake and fan were digitized along with the microphone signals.

The time domain ensembles were extracted, using the tachometer channels, so as to be synchronous with the rotation of the fan and with the rotation of the rake. Each ensemble was defined to start at the beginning of the fan revolution closest to the beginning of the corresponding rake revolution. Ensemble number 1 contained rake revolutions 1 to 5. Ensemble number 2 contained rake revolutions 2 to 6, and so on. These ensembles were then averaged together to improve the signal to noise ratio. A Hanning window function was applied after averaging.

The data storage requirements for this experiment became burdensome quite rapidly. Each test condition required storage of 640K samples (1.280 Mbytes) per data channel. There were five rake transducers, two tachometer channels and two rake immersions, giving a total data storage requirement for each test condition of 17.92 Mbytes (1.280 Mbytes * 7 channels * 2 immersions). Over 50 test conditions were run, resulting in data storage exceeding 900 Mbytes for raw files alone.

The spectral analysis for this data required computation of a Discrete Fourier Transform (DFT) with 160 000 points. This analysis does not allow direct application of the classic FFT algorithm, since 160 000 is not a power of 2. Instead, a chirp-Z transform was used. This technique allows for calculation of a complex spectrum more quickly than the "brute force" method employing the definition of the DFT. Even so, each chirp-Z transform required computation of three 256K-point FFTs. The computer used to perform this analysis was the TRADAR-3 system at NASA Lewis. The chirp-Z transform algorithm was taken from Ref. 6 and modified to use the TRADAR-3 vector accelerator hardware for FFT calculations.

Figure 1 shows a typical spectrum from the circumferential analysis. As discussed previously, each m-mode generates a tone at a distinct frequency. The spectrum in the figure, centered at the blade passing tone (16 shaft orders), contains 6 peaks. These peaks represent the magnitudes of circumferential modes of order -8, -4, 0, +4, +8, and +12. These modes are all multiples of 4, as expected for this configuration, which had four inlet rods. The extraneous tone due to the wake rake is located at mode +16.

Radial Mode Analysis

The algorithm used to compute the radial mode coefficients was originally developed in Ref. 7. The results are summarized here for convenience. The output from the circumferential analysis consists of a complex pressure value for each m-mode at nine different radial locations. The basic task performed by the radial analysis program is to calculate a least-squares curve fit using Bessel eigenfunctions to match this data. This yields the (complex) radial mode coefficients.

In an annular duct with uniform axial flow, the following expression may be derived from the separated acoustic wave equation to describe the modal shape of the sound field:⁷

$$p(\theta, r, x, t) = P_{m,n,f} E_{mn}(k_{mn}) \exp[i * (2 * \pi * f * t + m * \theta \pm \gamma_{mn} * x)] \quad (9)$$

where

f	temporal frequency
θ	circumferential angle
m	circumferential mode number
n	radial mode number
γ	axial wave number
r	radial distance normalized on outer duct radius
x	axial location
k_{mn}	eigenvalue (see below)

$E(k_{mn}r)$ is the radial mode function formed from J and Y type Bessel functions:

$$E(k_{mn}r) = C_{mn} [J_m(k_{mn}r) + Q_{mn} Y_m(k_{mn}r)] \quad (10)$$

Values for Q_{mn} and k_{mn} are determined by the duct inner and outer boundary conditions. With a hard walled duct, there must be a zero radial gradient at the wall, so:

$$J'_m(k_{mn}) + Q_{mn} Y'_m(k_{mn}) = 0 \quad (\text{Outer wall}) \quad (11)$$

and

$$J'_m(k_{mn}\sigma) + Q_{mn} Y'_m(k_{mn}\sigma) = 0 \quad (\text{Inner wall}) \quad (12)$$

Where σ is the ratio between inner and outer duct wall radius. The factor C_{mn} above is a normalizing constant which insures that the integral of power

squared across the duct is unity. The value of C_{mn} is given by:

$$\frac{1}{(C_{mn})^2} = \frac{\pi}{2} * \left\{ \left[1 - \left(\frac{m}{k_{mn}} \right)^2 \right] * \left[J_{mn}(k_{mn}) + Q_{mn} Y_m(k_{mn}) \right] - \left[\sigma^2 - \left(\frac{m}{k_{mn}} \right)^2 \right] * \left[J_{mn}(\sigma * k_{mn}) + q_{mn} Y_m(\sigma * k_{mn}) \right] \right\} \quad (13)$$

The general form of the mode pressure phasor in one axial plane is given by the following, where n is the radial mode order:

$$P_{m,r,f} = \sum_{n=0}^{\infty} P_{m,n,f} * E_{mn}(k_{mn}r) \quad (14)$$

In the case being considered here, a finite number of radial modes are assumed to exist, placing an upper bound on the value of n in the above. The output from the circumferential decomposition corresponds to the left hand side of Eq. (14). Calculation of the $P_{m,n,f}$ terms may be performed using a least-squares curve fit, minimizing the total mean square error, which is defined as follows:

$$\text{error}^2 = \sum_{i=1}^{N_p} \left[\sum_{n=0}^{N_m} P_{m,n,f} * E_{mn}(k_{mn}r_i) - P_{m,r,f} \right]^2 \quad (15)$$

where

N_m maximum radial mode order to compute

N_p number of radial measurement locations

m circumferential mode number

Matrix algebra is used to compute values for the radial mode coefficients such that the mean square error across all of the radial measurement locations is minimized. The results can be substituted back into a modified form of Eq. (14) to obtain an overall curve fit for each circumferential mode. Figure 5 shows a plot of the magnitude of the experimental data from a typical test condition together with corresponding results from the curve fit.

Figure 6 shows a three-dimensional magnitude plot of all the active radial/circumferential modes for one model configuration (one particular combination of inlet length and stator vane number) at a speed of 11 400 rpm. Plots of this type were used to evaluate the relative significance of various modes and to develop a better appreciation of the complexity of the modal content of the ADP model.

Analysis of Experimental Errors

The data measured using the rotating rake method contains both desired (signal) and undesired (noise) components. The desired signal is the true acoustic pressure generated by the fan. The undesired noise consists of all other unsteady pressures, such as turbulence, and/or electronic noise. The following section will discuss the development of procedures to choose the maximum radial mode during curve fitting, and the effect of noise contamination on the circumferential/radial mode analysis. Finally, the effect of the rake speed control system will be discussed.

Selecting the Number of Radial Modes

When performing the curve fit to obtain the radial coefficients, some method must be found to determine a correct upper limit on the number of radial modes. The maximum radial mode which can actually propagate is limited by the duct dimensions and flow conditions.^{8,9} In the ideal case, the circumferential decomposition will contain only signal and no noise. The mean square error defined in Eq. (15) will then become zero when the correct number of radial modes is used. In reality, the circumferential decomposition will contain some noise. This noise will require the use of extraneous, high ordered radial mode coefficients to obtain a low value for mean square error. Mean square error may be made arbitrarily close to zero if the number of radial modes is made equal to the number of radial pressure measurement locations. During the development of the data analysis software, some of the early attempts at curve fitting did use the maximum number of radial modes.

Table 1 shows the radial mode coefficients for a typical test case using actual experimental data. The curve fitting program was used, with the number of radial modes varying from 2 to 8. It appears that the "correct" solution would include radial modes 0, 1, and 2 (this conclusion is based partly on cutoff ratio, which is described below). The data for trials with five or more radials shows that the magnitude of some of the higher ordered coefficients became quite large. This incorrect result, which was typical for cases run using a large number of radials, prompted some further analysis.

The curve fitting program was modified to accept user inputs for radial mode coefficients and compute a pressure profile for the desired circumferential mode. This is the inverse of the normal operation for this program (given a circumferential distribution, compute the radial coefficients). The radial coefficients computed using the nine standard transducer locations were fed in. Circumferential pressures were computed for 50 evenly spaced radial distances, spanning the full radius of the duct. Thus, the radial coefficients determined by curve fitting through the nine transducer locations were used to predict the modal pressure shape across the entire duct.

Figure 7 shows the magnitude of the 9-point experimental data together with three 50-point curve fits. In the case using five radials, curve fit results for locations outside the standard transducer positions were reasonable, i.e., the magnitude did not show any large excursions. Results using eight radials were questionable, showing a large increase in predicted pressure near the hub. The results with nine radials were quite erroneous. While the curve fit was an exact match for the experimental data at the transducer locations, the predicted pressure near the hub became very large and unrealistic.

Calculation of Cutoff Ratio

Analysis of several cases like the one described above lead to a requirement to predict the "best" number of radial modes to use for curve fitting each case. An algorithm was developed to calculate a duct cutoff ratio for each potential mode. The basis for this calculation may be found in Ref. 9. The final form of the equation is as follows:

$$CR = \frac{n * B * M_t}{k_{mn}} * \left(1 - M_d^2\right)^{1/2} \quad (16)$$

where

n	BPF harmonic
B	number of blades
M_t	rotor tip Mach number
k_{mn}	eigenvalue for a particular circumferential (m) and radial (n) mode
M_d	Mach number at the duct wall, at the axial location of the rotating rake

The following procedure was developed for analyzing experimental results; Let Q equal the highest radial mode number where the cutoff ratio is equal to or greater than 1. Then calculate a curve fit using $Q + 1$ radial modes. If the magnitude of the $Q + 1$ order

radial coefficient is small (roughly one-half the size or smaller) compared to the other coefficients, the curve fit is acceptable. Other factors were considered as well. The normalized relative vector error (phase/magnitude) at each transducer location was calculated and examined as well. In general, the selection of the proper number of radial modes requires the application of some engineering judgement.

Quantitative Effect of Random Noise in Spectral Results

The technique described above for selecting the number of radial modes was developed using various test cases, such as the one to be described here. An artificial pressure profile was generated using the curve fit program with $m = 8$. These numbers are approximately the same as one of the experimental cases. The artificial pressure profile was distorted using various levels of additive white noise. The Signal to Noise Ratio (SNR) varied from +20 to -3 dB. For each case, a curve fit was computed using the first three radials. The resulting radial coefficients are shown in Table 2.

Figures 8 and 9 show the magnitudes of the resulting curve fits. These results (and others not documented here) suggest that SNR values in the 6 to 10 dB range are a minimum requirement to obtain an accurate curve fit. During analysis of the experimental data, the ratio between background level and tone peak level was examined to estimate actual SNR for each circumferential mode. Cases that were used to attempt to predict far field acoustic levels were selected using a minimum SNR of approximately 6 dB.

Rake Control System and Digitizing Errors

Two additional error sources that required monitoring were rake/fan position variations and digitizing clock rate.

During testing, speed variations in the fan were detected by the rake control system and compensatory changes in rake speed occurred automatically. These speed adjustments were not instantaneous, and not always 100 percent effective. The actual performance was monitored during data analysis. The rake and fan were each equipped with once-per-revolution tachometer pickups. These signals were digitized, along with the pressure transducers, using the angle clock. The number of samples between the occurrence of the rake once-per-revolution and the nearest fan once-per-revolution was calculated for each rake revolution. Ideally, this time differential would be constant, indicating tight synchronization (the fan should return to the same angular

position at the start of each rake revolution). Cases where the synchronization was poor were either redigitized from analog tape, or not used for radial mode decomposition.

When the data were digitized using the angle clock, the fan speed variations would sometimes cause the angle clock to generate 127 or 129 pulses per fan revolution instead of the desired 128. The data analysis software had a feature to count the number of samples between each fan once-per-revolution tachometer pulse. The number of samples between each rake tachometer pulse was also counted. During the analysis, the software generated a report on these counts to warn the operator of loss-of-sync events. Usage of rake data with serious loss-of-sync was minimized based on these reports.

The detection of data with more or less than the desired number of samples per revolution (128) is a simplistic check on synchronous digitizer performance. A better method would be to sample at a rate several times higher than the minimum of 128 samples per revolution. This would allow more accurate detection of loss-of-sync. One drawback to this approach would be larger data file storage requirements. Tachometer systems generating more than one pulse per revolution would also be helpful.

Lessons Learned/Recommendations for Future Research

Two difficulties that were encountered during rotating rake testing with the ADP model could be addressed in future experiments. The first difficulty was related to data acquisition and processing. The second difficulty involves the characteristics of the ducted fan model itself. This section concludes with some general comments on the selection of rake transducer locations and fan/rake speed ratio.

Rotating rake data from the ADP model was recorded on analog tape and played back later using an angle clock to control digitizing. This procedure was tedious and inefficient. It is recommended that future programs provide for on-line digitizing of the transducer signals during testing, assuming no adverse impact on the time required for data acquisition. A high speed/multichannel A/D computer system would be required. In place of the angle clock, the model should be designed to provide the digitizing control signal. For example, the fan shaft could be provided with an encoding device to generate 128 or more pulses per revolution. This signal could then be conditioned and used to drive the A/D converter directly.

The use of a fan having many propagating modes results in a complicated far field acoustic directivity. This does not detract from the validity of the rotating rake measurements, however, one goal in the development of computational aero-acoustics is to predict far field acoustic radiation given the in-duct modal coefficients. The rotating rake experimental data will be used to verify computational aero-acoustic results and/or improve computational models. The comparison between measured and predicted data becomes more difficult when many modes are propagating. A future test could be conducted where the fan is designed to allow only a few selected modes to propagate. This would simplify the near-field to far-field comparison task considerably.

Selection of the number and location for the rake transducers has, in the past, been done empirically. Reference 4 (Cicon, Sofrin, and Mathews) suggests the use of a number of transducers equal to twice the highest radial order that is expected. Reference 7 (Moore, JS and V) recommends that transducers be spaced in equal increments of duct radius squared, thus providing equal coverage of duct area. The rotating rake apparatus for this test provided nine radial measurements as described above. Analysis of the test cases at BPF were, for the most part, successful. If the radial content at higher harmonics of the blade passing frequency is of interest, more resolution is needed. During the ADP experiment, some analysis of data at $2 * \text{BPF}$ was performed. It was limited (typically) to cases where radial modes of order 4 or less were present.

Experience gained in the ADP test program suggests that the best method is an iterative process. The initial estimate for the number of transducers should be based on Ref. 4, with initial locations based on Ref. 7. This configuration would then be evaluated by simulating the in-duct pressure variations, inputting modal coefficients and additive noise. The sensitivity of the curve fitting process to noise level would be evaluated, and changes in microphone number and/or location could be proposed. Further simulation studies would then be conducted to optimize the rake design. The same computer program which was used to analyze the ADP data has the capability to perform this analysis.

The rake/fan speed ratio is another important parameter in the design of a rotating rake experiment. Rake speeds which are high compared to the fan speed are desirable to provide a greater frequency spread between adjacent tones. In some cases, the rake drive motor will be the limiting factor. Another limit exists as well. Referring back to Eq. (3), consider the frequencies of the following two tones (B = number of blades):

(1) One caused by a circumferential mode of order $+B$ at BPF. This is the highest-frequency tone in the cluster near BPF for subsonic tip speed.

(2) One caused by a circumferential mode of order $-2B$ at 2BPF. This is the lowest-frequency tone in the cluster near 2BPF for subsonic tip speed.

As rake speed is increased, a point will be reached where these two tones interfere with each other. This speed is the maximum upper limit for the case of subsonic tip speed. In cases with supersonic tip speed, modes of order greater than B may propagate. The maximum rake speed must be decreased accordingly.

Concluding Remarks

Testing of the ADP model in the NASA Lewis 9- by 15-Foot Low Speed Wind Tunnel included the first successful attempt to measure the inlet acoustic modes of a ducted fan using a rotating rake apparatus. This technology is significant for the following reasons:

1. The mechanisms controlling the generation of ducted fan acoustic modes can be investigated in an efficient manner, with rake intrusion effects minimized. A better understanding of these mechanisms can be used to develop more accurate computational models to predict the modal content.

2. The computational models describing acoustic mode propagation can be improved by performing a comparison between actual and predicted results for far-field acoustic levels.

The improved computational models can then be used to predict the acoustic performance of new aircraft engine systems during the early design phase, thus shortening development time and minimizing development costs.

The following improvements are recommended for future rotating rake experiments:

1. Use on-line digital data acquisition to analyze the rake pressures rather than analog tape recording. If data is to be digitized at a rate of 128 samples per fan revolution (for example), then install a 128-per-revolution shaft encoder on the fan.

2. Use a ducted fan with a simple acoustic mode signature, i.e., only one or two modes active at any time. A large, low speed fan rig is suggested, with inlet rods as needed to select the cut-on modes. This change will

facilitate the verification of computational aero-acoustic predictions.

3. Select the rotating rake drive motor to allow operation at maximum rake speed, subject to the limit imposed by interference between adjacent BPF harmonics. This will reduce the requirement for extremely fine spectral resolution and large computer data files.

References

1. Woodward, R.P., Bock, L.A., Heidelberg, L.J., and Hall, D.G., "Far-Field Noise and Internal Modes From a Ducted Propeller at Simulated Aircraft Takeoff Conditions," AIAA Paper 92-0371, Jan. 1992. (Also, NASA TM-105369, 1992).
2. Heidelberg, L., and Hall, D., "Acoustic Mode Measurements in the Inlet of a Model Turbofan Using a Continuously Rotating Rake," to be published as AIAA Paper 93-0598, 1993.
3. Sofrin, T.G., "Some Modal-Frequency Spectra of Fan Noise," AIAA Paper 81-1990, Oct. 1981.
4. Cicon, D.E., Sofrin, T.G., and Mathews, D.C., "Investigation of Continuously Traversing Microphone System for Mode Measurement," NASA CR-168040, 1982.
5. Konno, K.E., and Hausmann, C.R., "Rotating Rate Design for Unique Measurement of Fan-Generated Spinning Acoustic Modes," NASA TM-105946, Jan. 1993.
6. Stearns, S.D., and David, R.A., Signal Processing Algorithms, Prentice-Hall, Inc., Englewood Cliffs, NJ, 1988.
7. Moore, C.J., "Measurement of Radial And Circumferential Modes in Annular and Circular Fan Ducts," Journal of Sound and Vibration, Vol. 2, Jan. 1979, pp. 235-256.
8. Tyler, J.M., and Sofrin, T.G., "Axial Flow Compressor Studies," SAE Transactions, Vol. 70, 1962, pp. 309-332.
9. Rice, E.J., Heidmann, M.F., and Sofrin, T.G., "Modal Propagation Angles in a Cylindrical Duct with Flow and Their Relation to Sound Radiation," AIAA Paper 79-0183, Jan. 1979. (Also, NASA TM-79030, 1979.)

TABLE 1.—MAGNITUDE OF RADIAL COEFFICIENTS

Radial order	Maximum radial mode in curve fit						
	2	3	4	5	6	7	8
0	12.97	13.33	12.68	12.62	12.50	11.98	11.20
1	12.12	13.91	14.76	13.24	13.79	19.29	34.45
2	33.97	33.12	32.39	35.20	37.44	35.44	23.03
3		8.05	9.09	5.17	5.67	15.15	47.62
4			4.45	2.92	4.45	10.71	43.83
5				5.64	6.27	4.81	23.98
6					2.66	5.72	32.55
7						4.82	15.20
8							16.1

TABLE 2.—EFFECT OF NOISE ON RADIAL COEFFICIENTS

SNR	Radial order	Magnitude of radial coefficient	Phase of radial coefficient
No noise	0	16.7 (Pa)	1.425 (rad)
	1	64.8	.350
	2	22.8	-.521
+20 dB	0	14.4	1.481
	1	62.8	.372
	2	21.5	-.449
+14 dB	0	18.2	1.431
	1	67.5	.407
	2	24.3	-.464
+10 dB	0	16.4	1.709
	1	71.9	.367
	2	25.4	-.628
+6 dB	0	10.0	1.042
	1	65.0	.370
	2	32.4	-.810
+3 dB	0	24.2	1.552
	1	90.6	.208
	2	16.5	-1.238
0 dB	0	25.9	2.738
	1	115.5	.948
	2	47.9	.158
-3 dB	0	8.8	1.020
	1	54.4	2.414
	2	72.2	.733

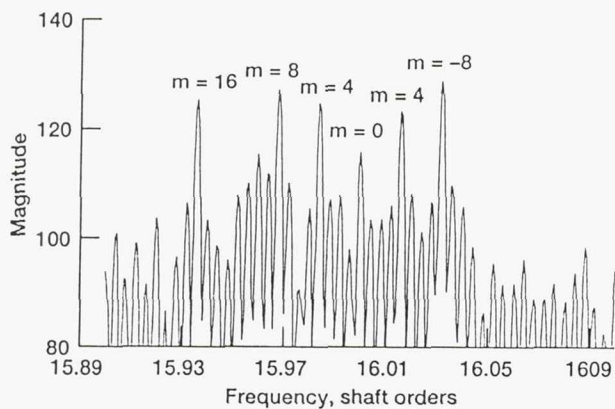


Figure 1.—Spectral data, 4-inlet rods, 10 800 RPM.

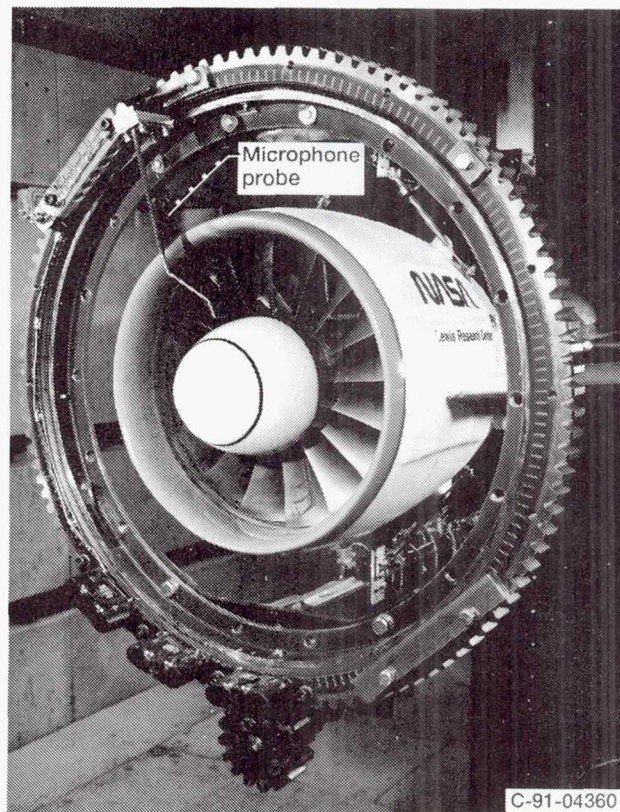


Figure 2.—Photograph of the ADP model in the 9X15 LSWT with rotating rake hardware installed.

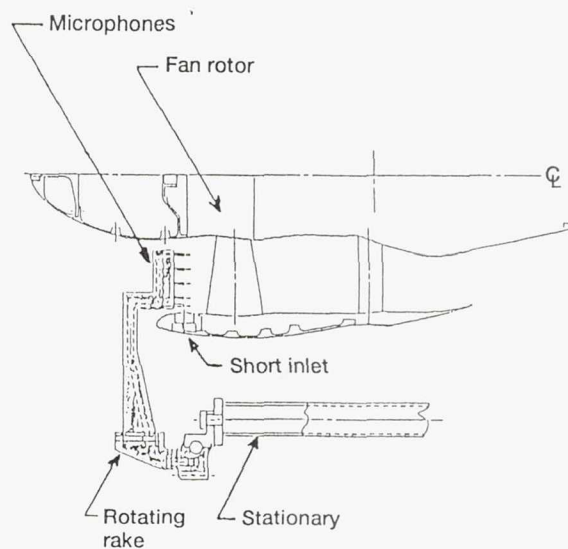
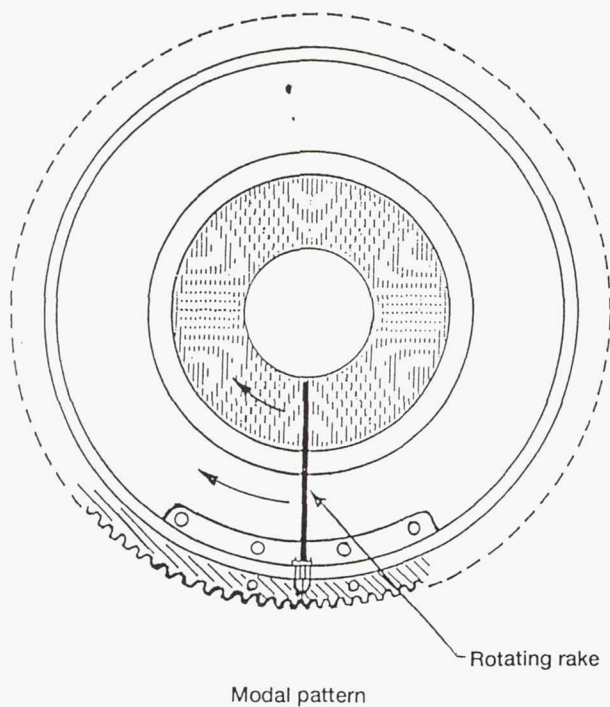


Figure 3.—Details of fan mode measurement rake.

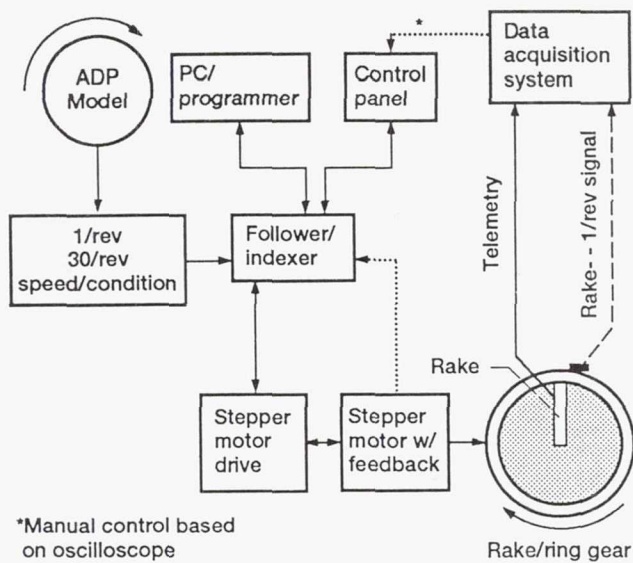


Figure 4.—Rotating rake system block diagram.

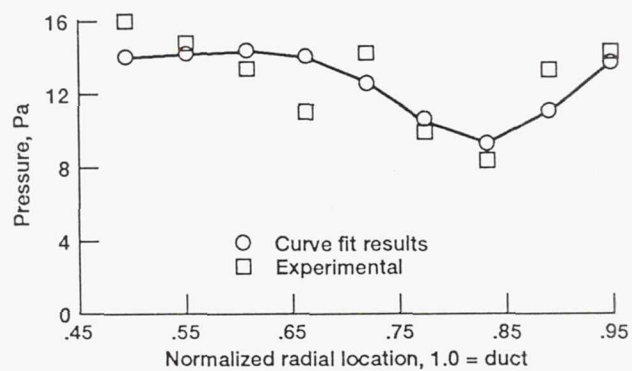


Figure 5.—Curve fit results, circum. mode 4, 3 radial.

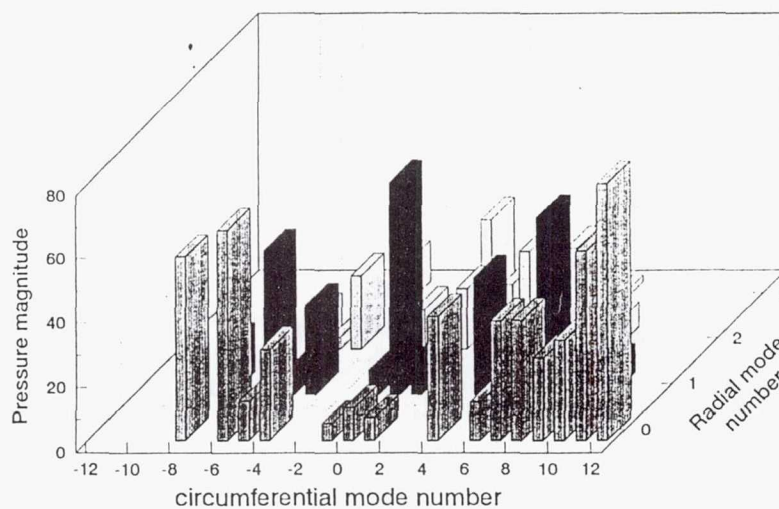


Figure 6.—Modal content for ADP model with long inlet and 22-vane stator at 11 400 RPM.

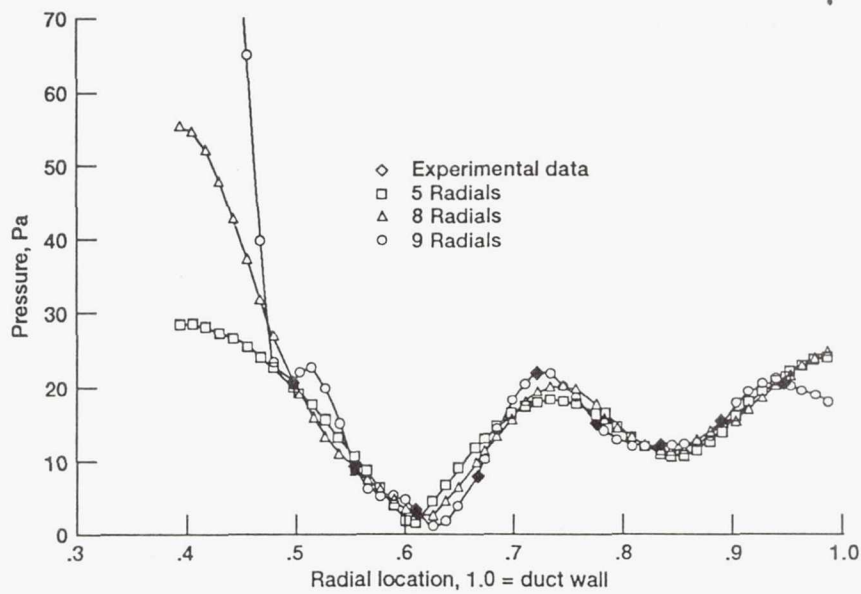


Figure 7.—Curve fit comparison.

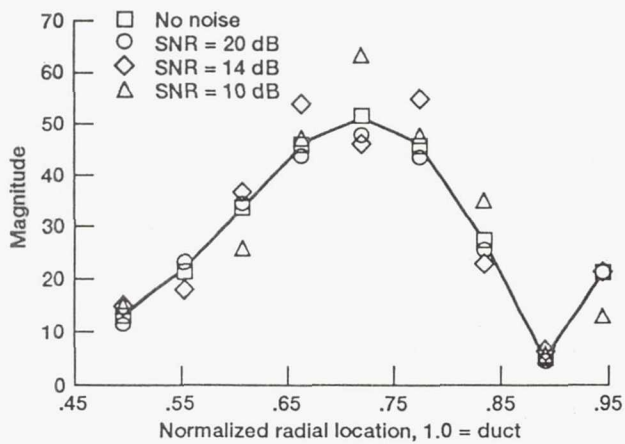


Figure 8.—Magnitude vs. SNR, curve fit results, $m = 8$.

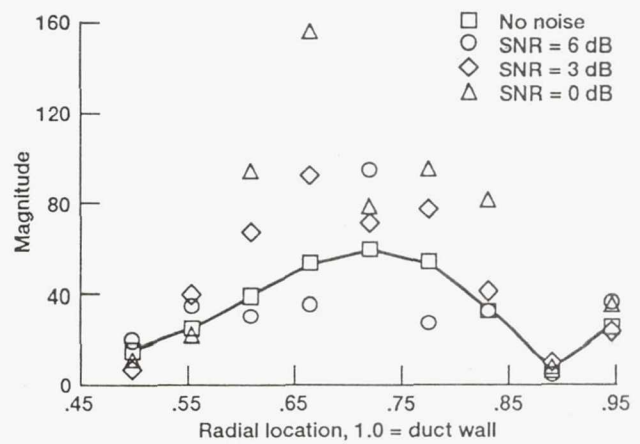


Figure 9.—Magnitude vs. SNR, curve fit results, $m = 8$.

REPORT DOCUMENTATION PAGE			Form Approved OMB No. 0704-0188	
Public reporting burden for this collection of information is estimated to average 1 hour per response, including the time for reviewing instructions, searching existing data sources, gathering and maintaining the data needed, and completing and reviewing the collection of information. Send comments regarding this burden estimate or any other aspect of this collection of information, including suggestions for reducing this burden, to Washington Headquarters Services, Directorate for Information Operations and Reports, 1215 Jefferson Davis Highway, Suite 1204, Arlington, VA 22202-4302, and to the Office of Management and Budget, Paperwork Reduction Project (0704-0188), Washington, DC 20503.				
1. AGENCY USE ONLY (Leave blank)	2. REPORT DATE January 1993	3. REPORT TYPE AND DATES COVERED Technical Memorandum		
4. TITLE AND SUBTITLE Acoustic Mode Measurements in the Inlet of a Model Turbofan Using a Continuously Rotating Rake: Data Collection/Analysis Techniques		5. FUNDING NUMBERS WU-535-03-10		
6. AUTHOR(S) David G. Hall, Laurence Heidelberg and Kevin Konno				
7. PERFORMING ORGANIZATION NAME(S) AND ADDRESS(ES) National Aeronautics and Space Administration Lewis Research Center Cleveland, Ohio 44135-3191		8. PERFORMING ORGANIZATION REPORT NUMBER E-7452		
9. SPONSORING/MONITORING AGENCY NAMES(S) AND ADDRESS(ES) National Aeronautics and Space Administration Washington, D.C. 20546-0001		10. SPONSORING/MONITORING AGENCY REPORT NUMBER NASA TM-105936 AIAA-93-0599		
11. SUPPLEMENTARY NOTES Prepared for the 31st Aerospace Sciences Meeting sponsored by the American Institute of Aeronautics and Astronautics, Reno, Nevada, January 11-14, 1993. David G. Hall, Sverdrup Technology, Inc., Lewis Research Center Group, 2001 Aerospace Parkway, Brook Park, Ohio 44142; Laurence Heidelberg and Kevin Konno, NASA Lewis Research Center. Responsible person, David G. Hall, (216) 433-3392.				
12a. DISTRIBUTION/AVAILABILITY STATEMENT Unclassified - Unlimited Subject Category 71, 7		12b. DISTRIBUTION CODE		
13. ABSTRACT (Maximum 200 words) This paper documents the rotating microphone measurement technique and data analysis procedures used to determine circumferential and radial acoustic mode content in the inlet of the Advanced Ducted Propeller (ADP) model. Circumferential acoustic mode levels were measured at a series of radial locations using the Doppler frequency shift produced by a rotating inlet microphone probe. Radial mode content was then computed using a least squares curve fit with the measured radial distribution for each circumferential mode. The rotating microphone technique is superior to fixed-probe techniques because it results in minimal interference with the acoustic modes generated by rotor-stator interaction. This effort represents the first experimental implementation of a measuring technique developed by T.G.Sofrin. Testing was performed in the NASA Lewis Low Speed Anechoic Wind Tunnel at a simulated takeoff condition of Mach 0.2. This paper includes the design of the data analysis software and the performance of the rotating rake apparatus. The effect of experimental errors is also discussed. The ADP model was designed and built by the Pratt & Whitney Division of United Technologies.				
14. SUBJECT TERMS Coherent fan noise; Acoustics; Measuring techniques			15. NUMBER OF PAGES 14	
			16. PRICE CODE	
17. SECURITY CLASSIFICATION OF REPORT Unclassified	18. SECURITY CLASSIFICATION OF THIS PAGE Unclassified	19. SECURITY CLASSIFICATION OF ABSTRACT Unclassified	20. LIMITATION OF ABSTRACT	

National Aeronautics and
Space Administration

Lewis Research Center
Cleveland, Ohio 44135

Official Business
Penalty for Private Use \$300

FOURTH CLASS MAIL

ADDRESS CORRECTION REQUESTED



Postage and Fees Paid
National Aeronautics and
Space Administration
NASA 451

NASA
